Published in final edited form as:
Virology. 2013 January 20; 435(2): 250–257. doi:10.1016/j.virol.2012.08.042.

Multiplicity-dependent activation of a serine protease-dependent cytomegalovirus-associated programmed cell death pathway

A. Louise McCormick[‡], **Linda Roback**, **Grace Wynn**, and **Edward S. Mocarski**
Department of Microbiology and Immunology and Emory Vaccine Center, Emory University School of Medicine, Atlanta GA 30322

Abstract

At a low MOI (≤ 0.01), cytomegalovirus-associated programmed cell death terminates productive infection via a pathway triggered by the mitochondrial serine protease HtrA2/Omi. This infected cell death is associated with late phase replication events naturally suppressed by the viral mitochondrial inhibitor of apoptosis (vMIA). Here, higher MOI (ranging from 0.1 to 3.0) triggers cell death earlier during infection independent of viral DNA synthesis. Thus, MOI-dependent activating signals early, at high MOI, or late, at low MOI, during replication promote serine protease-dependent death that is suppressed by vMIA. Treatment with an antioxidant targeting reactive oxygen species (ROS) or the serine protease inhibitor N-alpha-p-tosyl-L-lysine chloromethyl ketone (TLCK) delays cell death, and the combination has an additive impact. These studies identify serine proteases and ROS as important factors triggering programmed cell death induced by vMIA-deficient virus, and show that this death pathway occurs earlier and reduces viral yields as the MOI is increased.

Keywords

herpesvirus; apoptosis; HtrA2/Omi; serine-protease cell death; ROS; cytomegalovirus

Introduction

Programmed cell death is an evolutionarily ancient response to intracellular pathogens that is triggered by cell-intrinsic and cell-extrinsic signaling and follows caspase-dependent as well as caspase-independent pathways (Barber, 2001; Lamkanfi and Dixit, 2010; Mocarski et al., 2011). Human CMV (HCMV) and murine CMV (MCMV) inhibit caspase-dependent cell death (apoptosis) as well as other death pathways that have come to light through the study of virus-encoded cell death suppressors, that include some of the only evolutionarily conserved host modulatory functions retained by these two biologically similar but genetically divergent pathogens (Brune, 2011; McCormick, 2008; Mocarski et al., 2011). For some CMV cell death suppressors, mutant viruses trigger well characterized pathways. Thus, apoptosis triggered by activation of caspase-8 following infection is suppressed by the viral inhibitor of caspase-8 activation (vICA), encoded by HCMV UL36 or MCMV M36 (Cicin-Sain et al., 2008; McCormick et al., 2010; Menard et al., 2003; Skaletskaya et al.,

[‡]Corresponding author, Emory Vaccine Center, Emory University School of Medicine, 1462 Clifton Rd NE, Atlanta GA 30322, Phone: 404-727-9424, FAX: 404-712-9736, louise.mccormick@emory.edu.

2001). A novel programmed death pathway, referred to as cytomegalovirus-associated programmed cell death (cmvPCD) emerged from studies of vMIA encoded by HCMV UL37x1 (McCormick et al., 2008). This programmed cell death pathway is sensitive to serine protease inhibitor TLCK as well as the HtrA2/Omi inhibitor USF101 and proceeds independent of caspase activation. Although this death pathway takes place during infection with HCMV strain Towne*var*ATCC (Towne-BAC) (McCormick et al., 2005; McCormick et al., 2008), UL37x1 mutant viruses made from variants of strain AD169 have exhibited variable cell death patterns and replication defects that suggest the pathway is sensitive to differences in host cells and viral genetic background (Kaarbo et al., 2011; Reboredo et al., 2004; Sharon-Friling et al., 2006). In this report, we have used the inhibitor, TLCK, together with viral mutants to begin to understand how genetic differences and infection conditions impact cmvPCD and to dissect whether this pathway has the potential to impair viral replication as a component of host defense an important role of other programmed cell death pathways such as apoptosis (Lamkanfi and Dixit, 2010) and virus-induced necrosis (Upton et al., 2010, 2012).

At low MOIs (<0.1), cmvPCD is triggered late in infection and proceeds through a cellular process of fragmentation involving both the nucleus and cytoplasm (McCormick et al., 2008). This work revealed that infected human fibroblasts (HFs) undergo TLCK-sensitive cmvPCD independent of vMIA expression in a pattern that nonetheless demonstrated a natural role for this cell death suppressor in delaying the execution of cmvPCD. vMIA-deficient Towne-BAC virus (ΔUL37x1) was shown to undergo TLCK-sensitive cmvPCD approximately three days earlier than Towne-BAC at low MOI (<0.01) and vMIA-expressing HFs reversed this early pattern of death (McCormick et al., 2008). Thus, ΔUL37x1-induced cmvPCD begins on day 3 postinfection, with a frequency of ≤10%, and increases over 2 to 3 days, reaching 100% by day 5 to 6. In contrast, cmvPCD induced by parental Towne-BAC begins on day 6 postinfection and continues through day 10. Despite the earlier appearance of cell death, ΔUL37x1 virus produces similar yields of progeny and spreads cell-to-cell at a similar rate compared to Towne-BAC. cmvPCD is triggered by increasing levels of HtrA2/Omi (McCormick et al., 2008), a mitochondrial serine protease that contributes to both caspase-dependent and caspase-independent pathways, classically dependent on release from mitochondria (Vande Walle et al., 2008). Transient elevation of HtrA2/Omi levels within mitochondria promotes and overexpression of vMIA delays cmvPCD, suggesting a mechanism where mitochondrial localized vMIA maintains control over this pathway (McCormick et al., 2008). To address the trigger(s) that activate serine protease-dependent death during CMV infection, we evaluated the influence of MOI on timing of cell death. Importantly, these studies revealed MOI-dependent activation of cmvPCD more severely limits viral yields, emphasizing the role of cmvPCD as a host defense pathway. Input viral particles were insufficient to induce cmvPCD, however, a MOI-dependent timing of cell death was observed. At lower MOIs, initiation of cmvPCD was dependent on late replication events; whereas, viral immediate early or early gene products triggered cell death under higher MOI conditions. In addition to serine proteases, higher MOI revealed ROS-dependent control of cmvPCD, consistent with a role of HtrA2/Omi in regulation of oxidative stress (Krick et al., 2008). Thus, here we report that TLCK, a serine protease inhibitor, or BHA, an antioxidant can inhibit premature cmvPCD initiated by elevated multiplicity in the absence of vMIA.

Results

Dependence of intrinsic cell death controlled by vMIA on cell source and viral strain

To directly evaluate the potential role of cell source to differences in cell death induced by UL37x1 mutant viruses, we determined infectivity of Towne-BAC-derived ΔUL37x1 (McCormick et al., 2005) or AD169-BAC-derived RVHB5delUL37x1 (Reboredo et al.,

2004) following transfection. Consistent with previous reports, ΔUL37x1 virus (McCormick et al., 2005) was recovered from HFs but RVHB5delUL37x1 virus (Reboredo et al., 2004) was not (data not shown). ΔUL37x1 and RVHB5delUL37x1 viruses replicated on vMIA-HFs, however, plaque size and recovered titers indicated RVHB5delUL37x1 was more defective than ΔUL37x1 even in vMIA-complementing cells (data not shown). Overall, these results highlight genetic differences underlie replication properties of RVHB5delUL37x1 and ΔUL37x1. Cell source or culture conditions alone do not control differences in the replication properties of these viruses. Furthermore, the inability to completely complement RVHB5delUL37x1 replication in vMIA suggested that adventitious mutations may have accompanied the mutation of UL37x1 in this virus and contributed to decreased replication potential.

MOI-dependent intrinsic cell death pathways controlled by vMIA are induced at different stages of replication

To investigate the contribution of the input dose of virus to patterns of cell death and replication, vMIA-deficient ΔUL37x1 and Towne-BAC infections were carried out at MOIs of 1.0, 0.1 and 0.01 (Fig 1). As previously (McCormick et al., 2008), we relied on GFP fluorescence produced from these viruses as an initial, indirect indicator of viral yields. At MOI 1.0, fluorescence of ΔUL37x1-infected cultures was similar to Towne-BAC cultures early in infection (≤ 54 hpi), but was decreased relative to Towne-BAC at all late times evaluated (72–162 hpi) (Fig 1A–G). In contrast, at MOI 0.1, GFP fluorescence of ΔUL37x1-infected cultures remained equivalent to Towne-BAC through 90 hpi, decreasing only after 108 hpi (Fig 1H–N). At the lowest MOI (0.01), the fluorescence of ΔUL37x1-infected cells was weaker than Towne-BAC at late times (144–162 hpi) (Fig 1O–R). At this low MOI, equivalent foci were obvious by 120 hpi, consistent with our earlier characterization of this mutant virus that indicated differences between ΔUL37x1 and Towne-BAC emerge only after initial cell-to-cell spread (McCormick et al., 2005; McCormick et al., 2008). Overall, this evaluation revealed a multiplicity-dependent difference in fluorescence between ΔUL37x1 and the parental Towne-BAC, but, importantly, showed that the benefit of vMIA function(s) depends on the MOI employed.

To extend this analysis and evaluate differences in replication, yields from ΔUL37x1 and Towne-BAC virus were determined at daily intervals after infection at an MOI of 1 or 0.001 (Fig 2A). At the higher MOI, ΔUL37x1 yields stopped rising after 72 hpi, in striking contrast to the increase between 72 and 120 hpi with Towne-BAC. Mean titer values differed by 6- and 19-fold by 96 and 120 hpi, respectively, reaching statistical significance on both days. In comparison, mean titer values at low MOI differed by only 2.3 and 2.5 fold, respectively, at these same times, a value that, although statistically different at 96 hpi, was reduced in comparison to yields that followed infection at high MOI. Recently, impaired mitochondrial biogenesis in AD169-derived ΔUL37x1 has been correlated with a two-fold difference in viral titers, the expected result of the UL37x1-deficiency (Kaarbo et al., 2011). Here, emergence of GFP+ foci and cell death by 96–120 hpi (Fig 1 and data not shown), indicated the two-fold difference in viral yield at low multiplicity as well as the larger differences at higher multiplicity, would likely reflect the impact of multiple factors. Thus, we focused the remaining studies on cell death as well as viral replication.

To confirm the direct impact of vMIA function on replication at high MOI, HFs and HFs constitutively expressing vMIA (McCormick et al., 2005) were infected with ΔUL37x1 or Towne-BAC at MOI 3.0 (Fig 2B). ΔUL37x1 titers at 120 hpi were lower compared to Towne-BAC (≥ 50 fold) (Fig 2B), similar to differences at MOI 1.0 (Fig 2A). HFs transduced with vMIA complemented viral yields to Towne-BAC levels (Fig 2B), demonstrating a significant role for vMIA in viral replication. From fluorescence intensity patterns, emergence of cell-to-cell GFP+ cells or foci (Fig 1) and viral yields (Fig 2A–B), it

appeared that high MOI infection is associated with the induction of cell death at early times in a manner that is different from low MOI.

vMIA has been associated with suppressing cell death and as well, promoting endoplasmic reticulum calcium release and mitochondrial biogenesis during infection (Kaarbo et al., 2011; McCormick et al., 2008; Sharon-Friling et al., 2006). At low MOI Towne-BAC-derived ΔUL37x1 replication induces and vMIA suppresses a late phase event that triggers cell death (McCormick et al., 2008). Because higher MOI infection altered the timing and magnitude of GFP fluorescence and viral yield earlier during infection (Fig 1 and 2A–B), we re-evaluated timing and replication-phase specific contributions to premature cell death (Fig 2C–F). By Trypan Blue exclusion, approximately 50% of the total cells in ΔUL37x1-infected cultures (MOI of 1.0) remained viable 72–96 hpi, decreasing to less than 20% by 120 hpi. In comparison, Towne-BAC infected cultures remained fully viable through 120 hpi (data not shown). To determine whether the decreased viability reflected a loss of infected cells, viral immediate early (IE) nuclear antigen positive (IE+) cells were scored daily after infection (MOI of 1.0; Fig 2D). IE+ cell numbers in ΔUL37x1-infected cultures were highest at 24 hpi and decreased from 48 through 72 hpi (74% and 34%, respectively relative to 24 hpi), whereas IE+ cell numbers in Towne-BAC-infected cultures remained constant 24–72 hpi in Towne-BAC cultures. In combination, these analyses indicate that premature ΔUL37x-1-infected cell death contributes to lower viral yields.

Next, we compared the impact of the viral DNA synthesis inhibitor phosphonoformate (PFA), added from 1 hpi through 72, 96 and 120 hpi, on infection (Fig 2E). Given that GFP fluorescence is reduced during PFA treatment (McCormick et al., 2008), infection was scored by immunofluorescent detection of IE antigen (IE+) at 24, 72, 96 and 120 hpi (Fig 2E). Such treatment at low MOI does not result in cell death (McCormick et al., 2008). In contrast, IE+ cell number declined dramatically at higher MOI, falling to <10% viability by 120 hpi. Importantly, PFA blocked viral DNA replication independent of vMIA expression or MOI (data not shown). Overall, these data revealed that higher MOI ΔUL37x1-induced cell death was triggered by early events preceding viral DNA synthesis, whereas low low input doses resulted in death triggered via late events that follow DNA replication (McCormick et al., 2008).

Multiplicity-dependent replication (Fig 1–2A) and a shift in initiation of cell death from late phase to early phase (Fig 2E) suggest a relationship between particle dose and the requirement for vMIA function. Although the particle-to-PFU ratio of stock preparations used here were not assessed directly, HCMV strain Towne preparations have a reported particle-to-PFU ratio of approximately 100 (Stinski et al., 1979) consistent with observations here of decreased requirement for vMIA at multiplicities ≤ 1.0. To determine whether viral particles contributed to ΔUL37x1-induced cell death, UV-inactivated viral particles were added to low MOI ΔUL37x1 infections to mimic high MOI conditions (Fig 2F). Cell death was evaluated early (at 72 hpi) when ≤10% of infected cells have died under low MOI conditions (McCormick et al., 2008) and ≥50% of infected cells have died at an MOI of 1 (Fig 2C–D), thereby increasing the sensitivity of the assay. The addition of UV-inactivated UL37x1 or Towne-BAC particles made little impact on the ΔUL37x1-induced cell death (Fig 2F). As a measure of their biological activity, UV-inactivated particles were shown to increase levels of GFP fluorescence of ΔUL37x1-infected cells, but neither produced GFP+ signal or replicating virus when added to monolayers directly (data not shown). Thus, ΔUL37x1 induced cell death appears to be triggered by entry and early functions of replication-competent virus and not simply by the exposure to virus particles. Overall, these data indicate that infection at higher viral doses is accompanied by earlier cell death, in line with the observed replication differences between mutant and parental viruses.

Serine proteases and ROS promote premature cmvPCD of vMIA-deficient virus

In order to determine whether HtrA2/Omi triggers a serine protease-dependent cmvPCD pathway at high MOI as occurs at low MOI (McCormick et al., 2008), the inhibitor TLCK was added 24 hpi (MOI of 1.0) and cell death was scored when cell fragmentation was first apparent (48 hpi) (Fig 3A). TLCK treatment dramatically reduced the proportion of cells showing signs of death at 48 hpi. This protective impact correlated directly with the drug concentration, and, importantly, cell fragmentation was reduced by ≥ 85% at the highest drug concentration employed (100 μM). Thus, the cell death pathway induced by higher viral doses is dependent on serine proteases, as they have been implicated following low dose infection. The overall impact of the serine protease inhibitor, when applied at 24 h, improved, but did not fully restore, viral yields at 120 hpi (Fig 3B). We had previously evaluated HtrA2/Omi localization during low MOI infection (McCormick et al., 2008) that may dictate the initiation of cell death, but this remains to be explored in the high MOI setting. Overall, these data indicate that serine proteases control an important cell death pathway during infection that has the potential to cut short replication. Thus, vMIA-dependent suppression of this pathway may be viewed as crucial to the survival of virus-infected cells.

Because HtrA2/Omi can coordinate with caspases to regulate apoptosis (Vande Walle et al., 2008), and AD169 UL37x1 mutant virus can promote a zVAD-sensitive, caspase-dependent cell death (Reboredo et al., 2004), we evaluated whether caspases might be implicated here by using the pan-caspase inhibitor zVAD-fmk (Fig 3B). zVAD-fmk failed to prevent cell death at higher input doses of ΔUL37x1 (data not shown), consistent with unchanged viral yields in the absence of TLCK (Fig 3B). zVAD-fmk was ineffective regardless of concentrations ranging from 6–50 μM, doses sufficient to prevent cell death induced by staurosporine (data not shown). In combination, these data indicate that TLCK is an effective inhibitor of ΔUL37x1-induced cell death across a spectrum of virus doses. Based on these and previous studies (McCormick et al., 2005; McCormick et al., 2008), cmvPCD proceeds independent of caspases based on zVAD-resistance, regardless of the timing of cell death or influence of input virus dose. Here, viral yields indicated zVAD-fmk reduced the effectiveness of TLCK (Fig 3B); an unanticipated impact that we believe may indicate an off-target impact of zVAD-fmk. Overall, these studies implicate a serine protease-dependent death pathway controlled by vMIA regardless of ΔUL37x1 infection conditions.

To determine the role of ROS-dependent signaling during ΔUL37x1-induced cell death, the antioxidant butylated hydroxyanisole (BHA) was used to treat virus-infected cells (Fig 3C). Previous evaluations have indicated ROS-signaling regulates NF-κB- and AP-1-dependent transcription of the major IE promoter (Kim et al., 2005; Speir, 2000). To reduce impacts on IE gene expression, BHA was added from 6 hpi. Treatment with BHA reduced the levels of ΔUL37x1-induced cell death through 72 hpi. This suppression correlated directly with drug concentrations from 31 μM, reducing fragmentation by 35%, to 125 μM, reducing fragmentation by 85% (Fig 3C). BHA treatment alone was not sufficient to maintain infected cell viability through 96 hpi (Fig 3D and data not shown) or improve viral yields (Fig 3E). However, the drug did not interfere with Towne-BAC infection as indicated by culture ATP levels and viral titers (Fig 3D–E), suggesting, perhaps, that ROS production overcame the antioxidant or that an additional stress contributed to cell death 72 to 96 hpi. To evaluate whether BHA was sufficient to inhibit cell death early in replication and also, evaluate whether stress activated late in replication overcame the antioxidant, BHA was added together with the viral DNA synthesis inhibitor PFA (Fig 3F). BHA increased the proportion of IE+ ΔUL37x1-infected cells from <10% to >25% under these conditions, suggesting that ROS activity in the early phase of replication contributed to induction of cell death. Overall, these data reveal an antioxidant was sufficient to reduce ΔUL37x1-induced

cell death while TLCK was sufficient to reduce ΔUL37x1-induced cell death and increase yield.

ROS and serine proteases coordinately control cmvPCD at late times of infection

TLCK and BHA each inhibited premature cmvPCD by more than 85% at 48–72 hpi when added alone at 24 or 6 h, respectively, (Fig 3A, 3C, and data not shown) but lost effect by 96 hpi (Fig 3D and data not shown). To determine whether there is a single cell death pathway inhibited by both drugs or two independent cell death pathways, we evaluated the time of addition most effective for each drug in the control of cell death and whether the antioxidant and protease inhibitor provided a combinatorial impact that would extend infected cell viability to 96 hpi (Fig 4). Initially, we evaluated how late in infection BHA and TLCK could be added to suppress cell death (Fig 4A). TLCK and BHA added at 8 or 24 hpi inhibited premature cell death through 72 hpi, whereas, addition at 48 hpi was less effective. Thus, for either BHA or TLCK, cell death was reduced by > 90% when the inhibitors were added at 24 hpi. In contrast, BHA addition at 48 hpi had no effect and the impact of TLCK, although still significant, was reduced by > 25%. These results correlated with time of appearance of cmvPCD by 48–72 hpi (Fig 2) and are consistent with both drugs acting on a common pathway. Next, BHA and TLCK were added at 24 hpi in a checkerboard analysis with combinations of drugs varied across multiple concentrations (Fig 4B). BHA and TLCK had an additive effect on cell death at 96 hpi, over a multiple drug concentrations consistent with a common pathway. Whereas TLCK or BHA each had a modest effect, when combined the drugs decreased cell death by 30%. Thus, inhibiting the pathway controlled by the antioxidant and the serine protease inhibitor is sufficient to prevent cell death at 96 hpi. Overall, these data highlight the coordination of ROS and serine proteases in cmvPCD.

Discussion

In this report, we have shown that multiplicity of infection contributes to premature serine protease-dependent cmvPCD triggered by HCMV in the absence of vMIA. At the low multiplicity of 0.01, ΔUL37x1 replication follows the kinetics and, nearly, the amplitude of parental virus. At multiplicities ≥ 0.1 this virus fails to replicate efficiently due to the induction of premature cell death. The cmvPCD that occurs during Towne-BAC infection at any multiplicity tested takes place much later such that cell death does not compromise replication or yields. This unveils a crucial role for vMIA in counteracting death pathways that may terminate infection. The pathway promoting cell death at multiplicities ≥ 0.01 is initiated by the combined impact of particles and early phase events, while the cell death pathway activated at multiplicities ≤ 0.01 is initiated by late phase events. These results suggest that the cellular response(s) that influence whether the mutant virus induces cmvPCD may be determined by different stress or antiviral pathway(s) induced by increased particle load. Evidence suggests that HCMV infection induces interferon response pathways that are mirrored by application of UV-inactivated HCMV particles (Zhu et al., 1997), and we used UV-inactivated particles here to show that particle load alone, is insufficient to induce multiplicity-dependent cmvPCD; a result that leaves open the role(s) of stress or antiviral signaling pathways induced by virion components.

Irrespective of multiplicity, cmvPCD is sensitive to the serine protease inhibitor TLCK, consistent with our previous implication of serine proteases, including HtrA2/Omi, in cmvPCD. This protease is also likely to be important for the premature cell death at elevated multiplicity. In current studies, the pan-caspase inhibitor zVAD-fmk interfered with replication in the presence of TLCK, suggesting an off-target effect may preclude evidence for the role of caspases during ΔUL37x1 infection. As a result, the role of caspases in cmvPCD remains to be clarified. In addition to serine protease activity, the current studies revealed ROS as an important promoter of cmvPCD, since an antioxidant was sufficient to

inhibit cell death. These data are consistent with accumulating evidence of increases in ROS during infection (Kaarbo et al., 2011; Tilton et al., 2011) and activation of HtrA2/Omi in response to oxidant stress (Krick et al., 2008). Moreover, the effective concentration of TLCK required to inhibit cell death was reduced by ≥ 9 fold in the presence of the antioxidant, suggesting that ROS levels have a direct impact on levels of serine protease activity. Thus, these results indicate serine proteases and ROS contributed toward a single pathway activated at early times.

Mitochondria are the major cellular source of ROS, which is produced through oxidative phosphorylation. Although redox-dependent control of NF-κB- and p53-dependent signaling pathways may be of benefit to infection, in excess, ROS interfere with mitochondrial function and as a consequence promote organelle damage and cell death directly through both apoptotic and necrotic mechanisms (Hamanaka and Chandel, 2010; Holley et al., 2010; Krishna et al., 2011; Lamkanfi and Dixit, 2010; Murphy, 2009). In fact, both ROS and the cellular enzymes important to control ROS levels are reported to rise at late times of HCMV infection (Kaarbo et al., 2011; Tilton et al., 2011). In addition, previous studies have indicated the virus encodes functions that control oxidative stress, such as the β2.7 RNA that binds mitochondria respiratory complex I (Reeves et al., 2007). Together with evidence for elevated ROS and viral and cellular control mechanisms, our results here indicate that vMIA may be an important component of the viral program to control oxidative stress. Potential mechanisms for oxidative stress control may follow interactions with previously identified cellular proteins that facilitate vMIA-dependent modulation of mitochondrial function (Kaarbo et al., 2011; Poncet et al., 2006; Seo et al., 2011). Thus, the physical interactions of vMIA with viperin, an interferon-inducible protein, and with the mitochondrial phosphate carrier (PiC), a component of the ATP synthasome, have each been linked to reductions in cellular ATP levels and oxidative phosphorylation (Poncet et al., 2006; Seo et al., 2011) which may, as a result, reduce ROS levels. In contrast, infection-related increases in mitochondrial biogenesis and activity, and thereby ROS levels, have also been reported to be vMIA-dependent (Kaarbo et al., 2011). In sum, variable impacts on mitochondrial function currently prevent a direct correlation with the current study. The use of AD169BAC-derived viruses with different growth properties in previous studies and an inconsistent use of vMIA-expressing cells to demonstrate that the phenotype(s) observed result from the absence of vMIA and not some other inadvertent mutation introduced during mutant construction highlight potential confounding issues. In our current studies a direct comparison of RVHB5delUL37x1 (Reboredo et al., 2004) and ΔUL37x1(McCormick et al., 2005) revealed such unintended genetic differences, rather than cell source or methodology, is a major contributor to variable phenotypes of vMIA-mutant viruses. Overall, the role of vMIA in modulating mitochondrial activity and oxidative stress will benefit from further clarification. The results of the current study indicate these functions may overlap with pathways inducing premature cmvPCD. In summary, multiplicity, oxidative stress, and serine proteases emerge from these studies as determinants of cell death pathways controlling replication of vMIA-deficient HCMV.

Materials and Methods

Cells, viruses, and viral yield assays

Human fibroblasts (HFs) and vMIA-HFs were cultured as previously described (McCormick et al., 2005). The viruses ΔUL37x1 and Towne-BAC used in these studies have been characterized previously (McCormick et al., 2005; McCormick et al., 2008) and were derived from the BACmid clones Towne-BAC and ΔUL37x1 (Dunn et al., 2003) and maintained as DNA clones in *E. coli* or on complementing vMIA-HFs prior to experiments. The viruses RVHB5delUL37x1 and RVHB5 were obtained following transfection of

BACmid clones RVHB5delUL37x1 and RVHB5 maintained as DNA clones in *E. coli* or on complementing vMIA-HFs.

Viral yield and growth following transfection

For growth curves, HFs or vMIA-HFs were infected by ΔUL37x1 or parental Towne-BAC viruses in triplicate cultures, and yields were determined from total virus that included cell supernatant and sonicated infected cells (Sonicator 3000; Misomix, Inc., Farmingdale, NY). Titrations employed 0.16% pooled human gamma globulin (Baxter Healthcare, Deerfield, IL). Viral growth following transfection of BACmid DNA was assessed by live cell microscopy on days 7, 11, and 15.

Live cell imaging and fluorescence analysis of live cultures

Images from live cell cultures were obtained and analyzed as previously described (McCormick et al., 2005; McCormick et al., 2008). For purposes of determining fluorescence intensities, live cultures were analyzed at 37°C with Live Cell Imaging System IncuCyte FLR (Essen Bioscience, Inc, Ann Arbor, Michigan) with subsequent data analysis completed in Prism (Graphpad Software, La Jolla, CA).

Immunofluorescence staining assays

Immunodetection employed mouse monoclonal antibodies to viral nuclear antigens $IE1_{p72}$ and $IE2_{p86}$ (MAB 810, Chemicon, Temeculah, CA) and Texas Red-conjugated horse anti-mouse IgG (all from Vector, Burlingame, Calif.).

Impact of protease, kinase, and replication inhibitors on death and viral yield

Cells grown on coverslips in 24 well dishes or without coverslips in 96 well culture dishes were infected then fixed at varying times with 3.7% formaldehyde or 25% acetic acid in methanol, then permeabilized with Triton X-100 (EMD Biosciences, Darmstadt, Germany), stained with Hoechst 33258 (AnaSpec, San Jose, CA), and processed for microscopic evaluation as previously described or alternatively, infected cells were detached from culture dishes by trypsin and sonicated prior to titration on HFs. Alternatively, virus in supernatant was titered for some experiments. Cell numbers were determined directly by counting numbers of GFP+ cells or fragmented GFP+ cells by fluorescence microscopy, by counting numbers of Trypan Blue negative cells using a hemacytometer, following immunodetection, by counting numbers of viral nuclear antigens $IE1_{p72}$ and $IE2_{p86}$, comparing to untreated controls, or indirectly, by determination of intracellular ATP levels using the Cell Titer-Glo Luminescent Cell Viability Assay kit (Promega) according to the manufacturer's instructions. $IE1_{p72}$ and $IE2_{p86}$ positive cells were identified from fluorescent micrographs and counted directly or by CellProfiler software (Carpenter et al., 2006). Images were collected as previously described (McCormick et al., 2005; McCormick et al., 2008).

Inhibitors included TLCK (N-alpha-p-tosyl-L-lysine chloromethyl ketone) (Sigma, St. Louis, MO) and PFA (phosphonoformate) (Sigma, St. Louis, Mo) dissolved in water, and zVAD.fmk (Calbiochem, La Jolla, CA), staurosporine (Alexis Biochemicals, San Diego, CA), and BHA (butylated hydroxyanisole) (Sigma, St. Louis, MO) dissolved in DMSO (Sigma, St. Louis, Mo). Inhibitors were added by replacing culture medium with medium containing inhibitor while control medium included the appropriate solvent (DMSO) or no addition. DMSO does not impact death or CMV replication levels at the concentrations used (≤0.1%) (McCormick et al., 2005). Viral yield was determined from supernatant combined with sonicated cells as described above.

Statistical analyses

All data reported in text have been collected from experiments that have been repeated and are graphed as the mean with standard deviations determined within Microsoft Excel or Prism Graphpad. For purposes of determining statistical significance, data were analyzed in Prism Graphpad by unpaired t test.

Acknowledgments

This work was supported by PHS grant RO1 AI020211, awarded to Edward Mocarski, and Emory University Research Council funds awarded to A. Louise McCormick.

References

Barber GN. Host defense, viruses and apoptosis. Cell Death Differ. 2001; 8:113–126. [PubMed: 11313713]

Brune W. Inhibition of programmed cell death by cytomegaloviruses. Virus research. 2011; 157:144–150. [PubMed: 20969904]

Carpenter AE, Jones TR, Lamprecht MR, Clarke C, Kang IH, Friman O, Guertin DA, Chang JH, Lindquist RA, Moffat J, Golland P, Sabatini DM. CellProfiler: image analysis software for identifying and quantifying cell phenotypes. Genome biology. 2006; 7:R100. [PubMed: 17076895]

Cicin-Sain L, Ruzsics Z, Podlech J, Bubic I, Menard C, Jonjic S, Reddehase MJ, Koszinowski UH. Dominant-negative FADD rescues the in vivo fitness of a cytomegalovirus lacking an antiapoptotic viral gene. J Virol. 2008; 82:2056–2064. [PubMed: 18094168]

Dunn W, Chou C, Li H, Hai R, Patterson D, Stolc V, Zhu H, Liu F. Functional profiling of a human cytomegalovirus genome. Proc Natl Acad Sci U S A. 2003; 100:14223–14228. [PubMed: 14623981]

Hamanaka RB, Chandel NS. Mitochondrial reactive oxygen species regulate cellular signaling and dictate biological outcomes. Trends in biochemical sciences. 2010; 35:505–513. [PubMed: 20430626]

Holley AK, Dhar SK, St Clair DK. Manganese superoxide dismutase vs. p53: regulation of mitochondrial ROS. Mitochondrion. 2010; 10:649–661. [PubMed: 20601193]

Kaarbo M, Ager-Wick E, Osenbroch PO, Kilander A, Skinnes R, Muller F, Eide L. Human cytomegalovirus infection increases mitochondrial biogenesis. Mitochondrion. 2011; 11:935–945. [PubMed: 21907833]

Kim SJ, Varghese TK, Zhang Z, Zhao LC, Thomas G, Hummel M, Abecassis M. Renal ischemia/reperfusion injury activates the enhancer domain of the human cytomegalovirus major immediate early promoter. Am J Transplant. 2005; 5:1606–1613. [PubMed: 15943618]

Krick S, Shi S, Ju W, Faul C, Tsai SY, Mundel P, Bottinger EP. Mpv17l protects against mitochondrial oxidative stress and apoptosis by activation of Omi/HtrA2 protease. Proc Natl Acad Sci U S A. 2008; 105:14106–14111. [PubMed: 18772386]

Krishna S, Low IC, Pervaiz S. Regulation of mitochondrial metabolism: yet another facet in the biology of the oncoprotein Bcl-2. The Biochemical journal. 2011; 435:545–551. [PubMed: 21486225]

Lamkanfi M, Dixit VM. Manipulation of host cell death pathways during microbial infections. Cell host & microbe. 2010; 8:44–54. [PubMed: 20638641]

McCormick AL. Control of apoptosis by human cytomegalovirus. Current topics in microbiology and immunology. 2008; 325:281–295. [PubMed: 18637512]

McCormick AL, Meiering CD, Smith GB, Mocarski ES. Mitochondrial cell death suppressors carried by human and murine cytomegalovirus confer resistance to proteasome inhibitor-induced apoptosis. J Virol. 2005; 79:12205–12217. [PubMed: 16160147]

McCormick AL, Roback L, Livingston-Rosanoff D, St Clair C. The human cytomegalovirus UL36 gene controls caspase-dependent and -independent cell death programs activated by infection of monocytes differentiating to macrophages. J Virol. 2010; 84:5108–5123. [PubMed: 20219915]

McCormick AL, Roback L, Mocarski ES. HtrA2/Omi terminates cytomegalovirus infection and is controlled by the viral mitochondrial inhibitor of apoptosis (vMIA). PLoS pathogens. 2008; 4:e1000063. [PubMed: 18769594]

Menard C, Wagner M, Ruzsics Z, Holak K, Brune W, Campbell AE, Koszinowski UH. Role of murine cytomegalovirus US22 gene family members in replication in macrophages. J Virol. 2003; 77:5557–5570. [PubMed: 12719548]

Mocarski ES, Upton JW, Kaiser WJ. Viral infection and the evolution of caspase 8-regulated apoptotic and necrotic death pathways. Nature reviews. Immunology. 2011; 12:79–88.

Murphy MP. How mitochondria produce reactive oxygen species. The Biochemical journal. 2009; 417:1–13. [PubMed: 19061483]

Poncet D, Pauleau AL, Szabadkai G, Vozza A, Scholz SR, Le Bras M, Briere JJ, Jalil A, Le Moigne R, Brenner C, Hahn G, Wittig I, Schagger H, Lemaire C, Bianchi K, Souquere S, Pierron G, Rustin P, Goldmacher VS, Rizzuto R, Palmieri F, Kroemer G. Cytopathic effects of the cytomegalovirus-encoded apoptosis inhibitory protein vMIA. J Cell Biol. 2006; 174:985–996. [PubMed: 16982800]

Reboredo M, Greaves RF, Hahn G. Human cytomegalovirus proteins encoded by UL37 exon 1 protect infected fibroblasts against virus-induced apoptosis and are required for efficient virus replication. J Gen Virol. 2004; 85:3555–3567. [PubMed: 15557228]

Reeves MB, Davies AA, McSharry BP, Wilkinson GW, Sinclair JH. Complex I binding by a virally encoded RNA regulates mitochondria-induced cell death. Science. 2007; 316:1345–1348. [PubMed: 17540903]

Seo JY, Yaneva R, Hinson ER, Cresswell P. Human cytomegalovirus directly induces the antiviral protein viperin to enhance infectivity. Science. 2011; 332:1093–1097. [PubMed: 21527675]

Sharon-Friling R, Goodhouse J, Colberg-Poley AM, Shenk T. Human cytomegalovirus pUL37x1 induces the release of endoplasmic reticulum calcium stores. Proc Natl Acad Sci U S A. 2006; 103:19117–19122. [PubMed: 17135350]

Skaletskaya A, Bartle LM, Chittenden T, McCormick AL, Mocarski ES, Goldmacher VS. A cytomegalovirus-encoded inhibitor of apoptosis that suppresses caspase-8 activation. Proc Natl Acad Sci U S A. 2001; 98:7829–7834. [PubMed: 11427719]

Speir E. Cytomegalovirus gene regulation by reactive oxygen species. Agents in atherosclerosis. Ann N Y Acad Sci. 2000; 899:363–374. [PubMed: 10863553]

Stinski MF, Mocarski ES, Thomsen DR. DNA of human cytomegalovirus: size heterogeneity and defectiveness resulting from serial undiluted passage. J Virol. 1979; 31:231–239. [PubMed: 228055]

Tilton C, Clippinger AJ, Maguire T, Alwine JC. Human cytomegalovirus induces multiple means to combat reactive oxygen species. J Virol. 2011

Upton JW, Kaiser WJ, Mocarski ES. Virus inhibition of RIP3-dependent necrosis. Cell host & microbe. 2010; 7:302–313. [PubMed: 20413098]

Upton JW, Kaiser WJ, Mocarski ES. DAI/ZBP1/DLM-1 complexes with RIP3 to mediate virus-induced programmed necrosis that is targeted by murine cytomegalovirus vIRA. Cell host & microbe. 2012; 11:290–297. [PubMed: 22423968]

Vande Walle L, Lamkanfi M, Vandenabeele P. The mitochondrial serine protease HtrA2/Omi: an overview. Cell Death Differ. 2008; 15:453–460. [PubMed: 18174901]

Zhu H, Cong JP, Shenk T. Use of differential display analysis to assess the effect of human cytomegalovirus infection on the accumulation of cellular RNAs: induction of interferon-responsive RNAs. Proc Natl Acad Sci U S A. 1997; 94:13985–13990. [PubMed: 9391139]

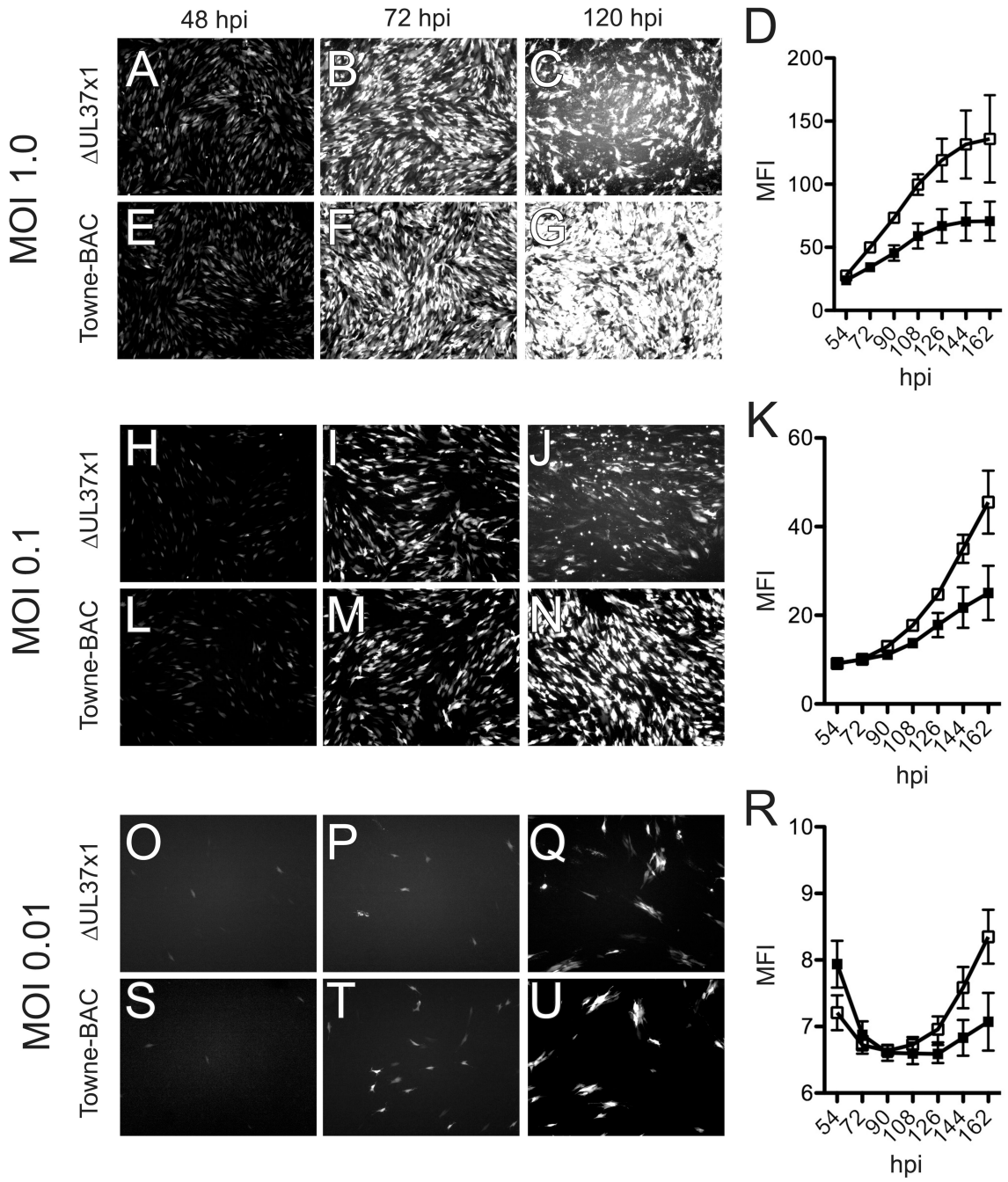

Figure 1. MOI-dependent impact on GFP fluorescence patterns of ΔUL37x1 and Towne-BAC viruses

Fluorescence micrographs and mean fluorescence intensities obtained from HF cells with GFP-expressing ΔUL37x1 or parental Towne-BAC viruses at an MOI of 1.0 (panels A–G), 0.1 (panels H-N), or 0.01 (panels O-U). Live cell images were collected by equivalent exposure times to illustrate differences in GFP+ fluorescence intensities, cell number, and cell-to-cell spread (original magnification 40X). Mean fluorescence intensity recorded by IncuCyte FLR imaging system from three independent wells infected with Towne-BAC (open symbols) or ΔUL37x1 (filled symbols) and graphed with standard deviation.

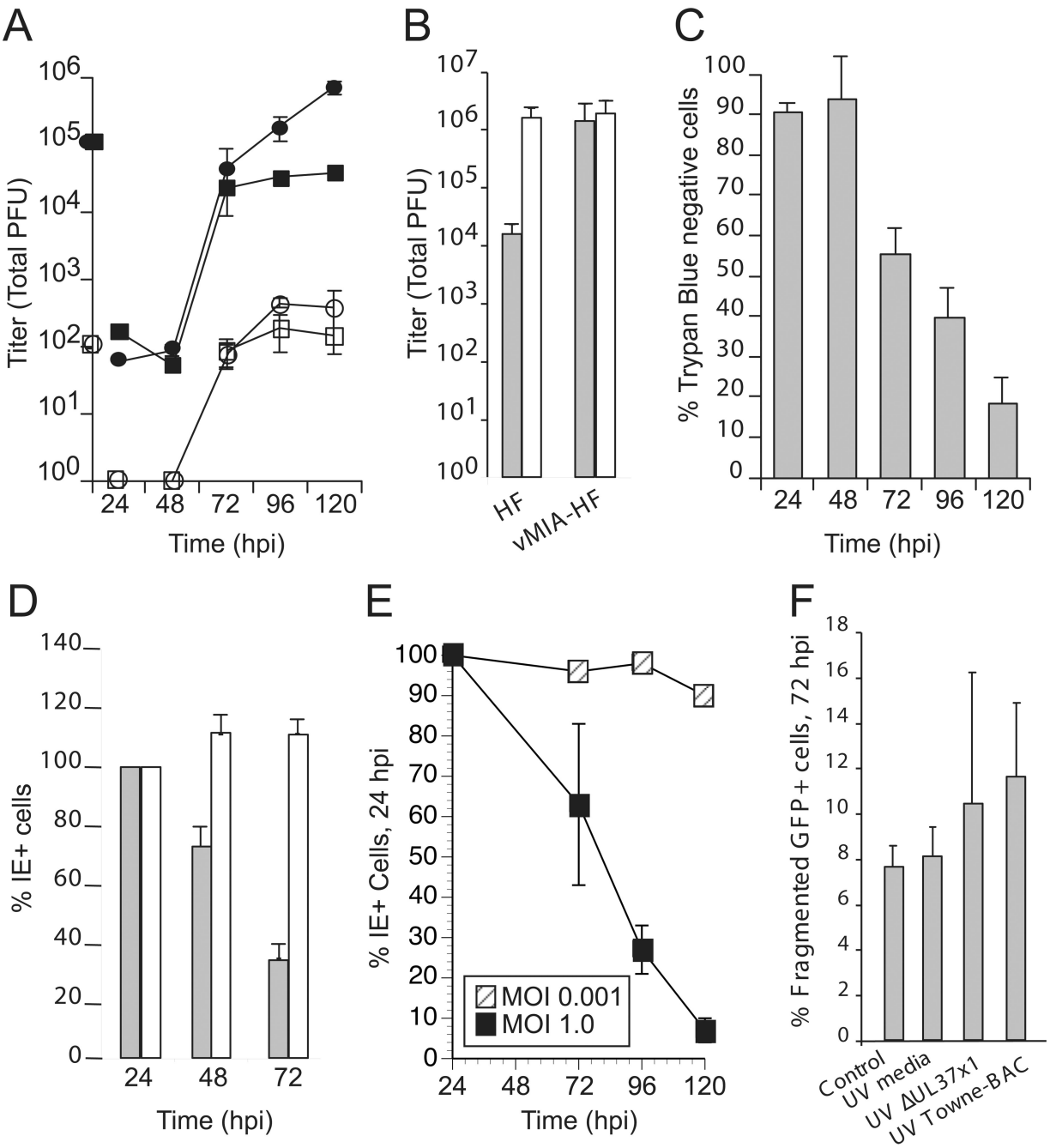

Figure 2. Impact of MOI on ΔUL37x1 virus replication and cell death patterns

A. Viral yields (titers, determined by plaque assay) of ΔUL37x1 (square symbols) or Towne-BAC (round symbols) after infection of HFs at MOIs of 1.0 (filled symbols) or 0.001 (open symbols). For MOI 1, 120 hpi, p= 0.0019. For MOI 0.001, 120 hpi, p = 0.4044. B. Mean viral yield at 120 hpi of HF or vMIA-HF cell cultures with ΔUL37x1 (gray bars) or Towne (open bars) (MOI 3.0). C. Percentage (%) of Trypan Blue negative cells (an indicator of viability) remaining in ΔUL37x1-infected cell cultures relative to Towne-BAC infected-cultures (MOI of 1.0). D. Percentage (%) of IE+ cells (an indicator of infection) in ΔUL37x1 (gray bars) or Towne-BAC (open bars) infected cultures relative to total IE+ cells at 24 hpi (MOI of 1.0). E. Percentage (%) of IE+ cells remaining in PFA-treated ΔUL37x1-

infected cultures relative to 24 hpi (depicted as 100%) following infection at an MOI of 0.001 (hatched square) or 1.0 (filled square). PFA was added at 300 μg/ml from 1 hpi. F. Percentage (%) of fragmented GFP+ cells at 72 hpi with ΔUL37x1 (MOI of 0.001) relative to total GFP+ cells. UV inactivated ΔUL37x1 or Towne-BAC were added at the equivalent of an MOI of 3.0 together with ΔUL37x1. UV treated mock medium or medium without addition served as controls. For all panels, the mean ± standard deviation (SD) represented by error bars is depicted.

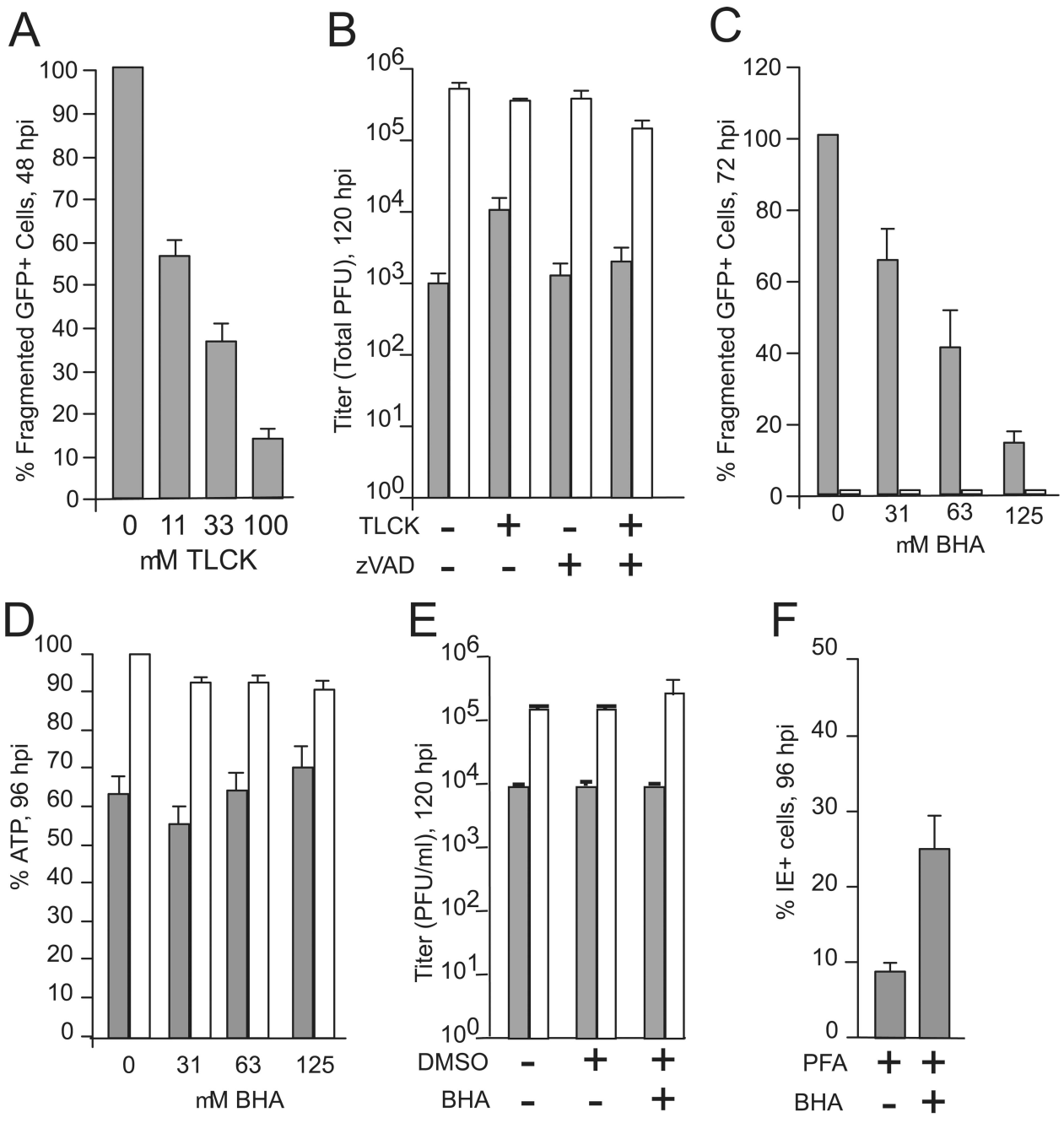

Figure 3. Serine protease- and ROS-dependent pathways contribute to premature cmvPCD

A. Percentage (%) of fragmented cells in ΔUL37x1-infected cultures (MOI of 1.0) at 48 hpi in the presence of serine protease inhibitor TLCK, applied from 24 hpi, relative to infection in the absence of the inhibitor. B. Viral yields (titers) from ΔUL37x1 (gray bars) or Towne–BAC (open bars) infected cells (MOI of 1.0) maintained in the presence of 33 μM TLCK, 25 μM zVAD-fmk, or both, from 24 to 120 hpi. C. Percentage (%) of fragmented cells at 72 hpi in ΔUL37x1 (gray bars) or Towne-BAC (open bars) infected cultures (MOI of 1.0) maintained in presence of BHA added from 6 hpi relative to untreated, infected cultures. D. Percentage (%) of ATP detected in ΔUL37x1 (gray bars) or Towne–BAC (open bars) infected cultures (MOI of 1.0) treated with BHA from 6 to 96 hpi relative to untreated

Towne-BAC-infected cultures. E. Viral yields (titer) of ΔUL37x1 (D) and Towne-BAC (E) (MOI of 1.0) released into supernatants in cultures maintained in 63 μM BHA from 8 to 120 hpi. F. Percentage (%) of IE+ cells remaining at 96 hpi in ΔUL37x1-infected cultures (MOI of 1.0) treated with PFA or a combination of PFA and BHA relative to Towne-BAC-infected cultures treated with PFA from 1 hpi. $p = 0.0002$.

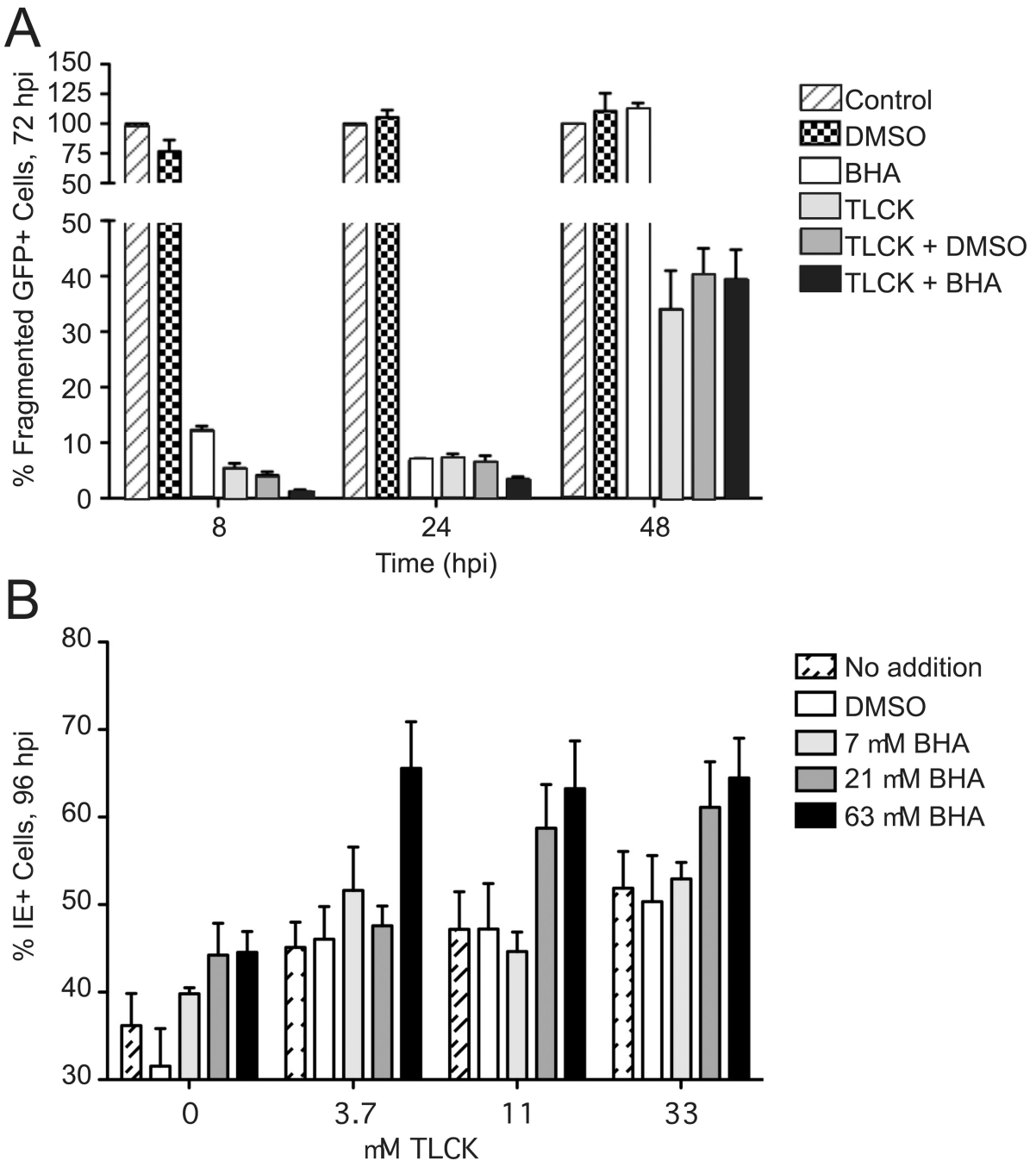

Figure 4. ROS- and serine protease-dependent events coordinate in control of cmvPCD

A. Percentage of fragmented cells in ΔUL37x1-infected cultures relative to control, mock-treated cultures (MOI of 1.0) maintained in 63 μM BHA, 33 μM TLCK, or both from 8, 24, or 48 to 72 hpi. Note: Medium replacement at 8, 24, or 48 hpi did not alter cell death (data not shown). BHA: $p < 0.0001$ (8 and 24 hpi). TLCK: $p < 0.0001$ (8, 24, and 48 hpi). B. Percentage (%) of IE+ cells remaining in ΔUL37x1-infected cultures maintained in BHA, TLCK, or both from 24 to 96 hpi relative to similarly treated Towne-BAC-infected cultures (MOI of 3.0). Solvent control (DMSO) was added at 0.01%. 3.7μM TLCK with 63 μM BHA, $p = 0.0237$.